JOURNAL GEOLOGICAL SOCIETY OF INDIA
Vol.87, March 2016, pp.271-286

Landslide Susceptibility Mapping Using Analytical Hierarchy Process (AHP) in Tehri Reservoir Rim Region, Uttarakhand

ROHAN KUMAR* and R. ANBALAGAN
Department of Earth Sciences, Indian Institute of Technology, Roorkee, Uttarakhand, India
***Email:** rohananadi@yahoo.com

Abstract: A comprehensive use of analytical hierarchy process (AHP) method in landslide susceptibility mapping (LSM) has been presented for rim region of Tehri reservoir. Using remote sensing data, various landslide causative factors responsible for inducing instability in the area were derived. Ancillary data such as geological map, soil map, and topographic map were also considered along with remote sensing data. Exhaustive field checks were performed to define the credibility of the random landslide conditioning factors considered in this study. Apart from universally acceptable inherent causative factors used in the susceptibility mapping, others such as impact of reservoir impoundment on terrain, topographic wetness index and stream power index were found to be important causative factors in rim region of the Tehri reservoir. The AHP method was used to acquire weights of factors and their classes respectively. Weights achieved from AHP method matched with the existing field conditions. Acceptable consistency ratio (CR) value was achieved for each AHP matrix. Weights of each factor were integrated with weighted sum technique and a landslide susceptibility index map was generated. Jenk's natural break classifier was used to classify LSI map into very low, low, moderate, high and very high landslide susceptible classes. Validation of the susceptibility map was performed using cumulative percentage/success rate curve technique. Area under curve value of the success rate curve was converted to percentage validation accuracy and a reasonable 78.7% validation accuracy was achieved.

Keywords: Landslide, Susceptibility, AHP, Reservoir rim, Tehri Dam, Uttarakhand

INTRODUCTION

There has been a noticeable increase in the number of natural disasters occurring worldwide causing huge loss of human life and property. Impact of natural disasters is amplified in the regions where topography is rugged and human settlements are remotely established. Anthropogenic activities, such as development of infrastructure, townships in environmentally sensitive zones have also amplified the impact of disasters as reflected from a number of events occurred in last few years. Some of the recent examples in this context can be given as Fukushima disaster in Japan (2012), Kedarnath disaster (2013) in Uttarakhand, India,. In the wake up of current events, proper planning and mitigation strategies are prerequisite for any government machinery responsible for development activities in a region. Present global scenario necessitates the identification of terrains vulnerable to natural disasters of an area. Susceptibility study for natural disasters of a region makes it easier to execute a planned infrastructure development. Present study area is situated in rugged lesser Himalayan terrain. Construction of Tehri dam and consequent development of a huge reservoir (67 km long) has substantially changed the nature of the terrain. After the impoundment of water in the reservoir, increased incidences of landslides have been reported from the rim region. Steep topography of the area, unfavourable lithology and structural discontinuities as well as nature of soil are the major reasons for the instability in the region. (Gupta and Anbalagan 1997; Kumar and Anbalagan 2013). Combination of reservoir side slope adjustment process and the inherent landslide causative factors are making Tehri reservoir rim area highly vulnerable to landslides. In general, landslides are caused by combination of geo-environmental factors which were discussed by Varnes (1984) and Hutchinson (1995). Most important inherent factors are bedrock geology (lithology, structure, degree of weathering), geomorphology (slope gradient, aspect, and relative relief), soil (depth, structure, permeability, and porosity), land-use/land-cover (LULC), and hydrologic conditions. Landslides are triggered by many extrinsic causative factors such as rainfall, earthquake, blasting and drilling, cloudburst, flash-floods etc. Gupta and Anbalagan (1997) used a set of inherent landslide causative factors namely: lithology, structural discontinuity, hydrogeology, slope morphometry, and LULC along with

external factors: seismicity and earthquake for landslide hazard zonation (LHZ) study in the Tehri reservoir rim region. According to Varnes (1984), zonation applies in general terms to division of the land surface into areas and ranking these areas according to the degree of actual or potential hazard from landslides or other mass movement on slopes. Landslide hazard is considered in natural hazard category which is defined as the probability of occurrence within a specified period of time and within a given area of potentially damaging phenomenon (Varnes 1984). Another definition of landslide vulnerability was given as the spatial probability of occurrence of landslide based on a set of geo-environmental factors (Brabb 1984). Several authors emphasised that susceptibility holds for 'where' landslide will occur whereas hazard stands for 'when' landslide will occur (Guzzetti et al. 1999; van Westen et al. 2006). In the present study, definition of landslide susceptibility was followed to carry out the identification of landslide prone zones (Fell et al. 2008).

A number of different methods are available to identify landslide susceptible zones. Several authors attempted to classify LHZ technique (Guzzetti et al. 1999; Aleotti and Chowdhury 1999; Guzzetti et al.2005; Kanungo et al. 2009). In general, landslide susceptibility methods can be grouped into the following three broad categories: qualitative, semi-quantitative and quantitative methods. Qualitative methods involve geomorphologic mapping approach, heuristic approach and other subjective judgement approach (Zimmerman et al. 1986; Anbalagan 1992; Nagarajan et al. 1998; Gupta et al.1999; Saha et al. 2002). Semi-quantitative methods consider weighing and rating based on logical tools such as AHP, fuzzy logic, combined landslide frequency ratio & fuzzy logic and weighted linear combination (WLC) (Ercanoglu and Gokceoglu 2004; Kanungo et al. 2006; Champatiray et al. 2007; Yalcin 2008; Pradhan and Lee 2009; Mondal et al. 2012; Kayastha et al. 2013). Quantitative landslide susceptibility methods produce numerical estimates (probabilities) of the occurrence of landslide phenomena in any hazard zone (Guzzetti et al. 1999). Quantitative methods are landslide inventory driven methods which predict landslide probability based on the assumption that landslide conditioning factors and landslides are uniformally distributed in an area. Quantitative methods are further divided into bivariate and multivariate classes. Bivariate landslide susceptibility method is based on link between historical landslide data and landslide density in factors (Dai and Lee 2002; Lee and Pradhan 2007; Mathew et al. 2007; Dahal et al. 2008; Pradhan and Lee 2010; Ghosh et al. 2011; Kumar and Anbalagan, 2013). It considers landslide as dependent variable whereas factors as independent variables and are considered individually for susceptibility assessment. Multivariate methods are also data driven but in this case, combined influence of factors on dependent variables are mathematically synthesized and influence of individual factors can also be acquired in numerical form (Lee 2005; Yesilnacar and Topal 2005; Lee and Pradhan 2007; Mathew et al. 2007; Pradhan and Lee 2010; Das et al. 2010; Das *et al.* 2012; Kundu et al. 2013). Another type of quantitative method is the deterministic method which is a site specific method. Deterministic method is based on geometric properties of slope, structural discontinuity, moisture content etc. This gives result in the form of factor of safety of particular slope (Sharma et al. 1995; Singh et al. 2008; Chakraborty and Anbalagan 2008).

A quantum of literature is available on LSM for the Uttarakhand Himalaya. Almost each methodology of susceptibility mapping was applied in this region (Saha et al. 2002; Arora et al. 2004; Kanungo et al. 2006; Champatiray et al. 2007; Mathew et al. 2007; Anbalagan et al. 2008; Das et al. 2010; Kundu et al. 2013). Review of the literature revealed that in general, each method is suitable for susceptibility mapping in this region. Some authors found multivariate statistical method more suitable (Das et al. 2012; Kundu et al. 2013) where as others found bivariate statistical method suitable (Saha et al. 2005). Heuristic methods such as LHEF (landslide hazard evaluation factor) based LHZ (which is also a Bureau of Indian Standards code) and GIS based weighted overlay approach were extensively applied in the Uttarakhand Himalayan region (Anbalagan 1992; Pachauri and Pant 1992; Gupta et al. 1999; Sarkar et al. 2004). But there still exist confusion about the use of a model which would be the best fit for the rugged Himalayan terrain. Varnes (1984) and Guzzetti et al. (1999) emphasised the use of heuristic models for the regional scale hazard zonation mapping. As the highly rugged lesser Himalayan terrain inherit steep spatial variation in lithology, structure, slope morphometry and drainage pattern, it is very sketchy to implement the exhaustive numerical susceptibility model in the field. Use of AHP model in the present region is also not found. This paper presents the use of the AHP method for weighing factors and their classes to generate a landslide susceptibility map of the rim region of Tehri reservoir.

STUDY AREA AND DATA PREPARATION

The area falls under longitude/latitude of 78.5° E and 30.5° N respectively (Fig. 1). Its administrative limits are covered within the domain of Tehri Garhwal district of Uttarakhand state. The area is covered in Survey of India topographic sheet no 53J/7 NW at a scale of 1:25000.

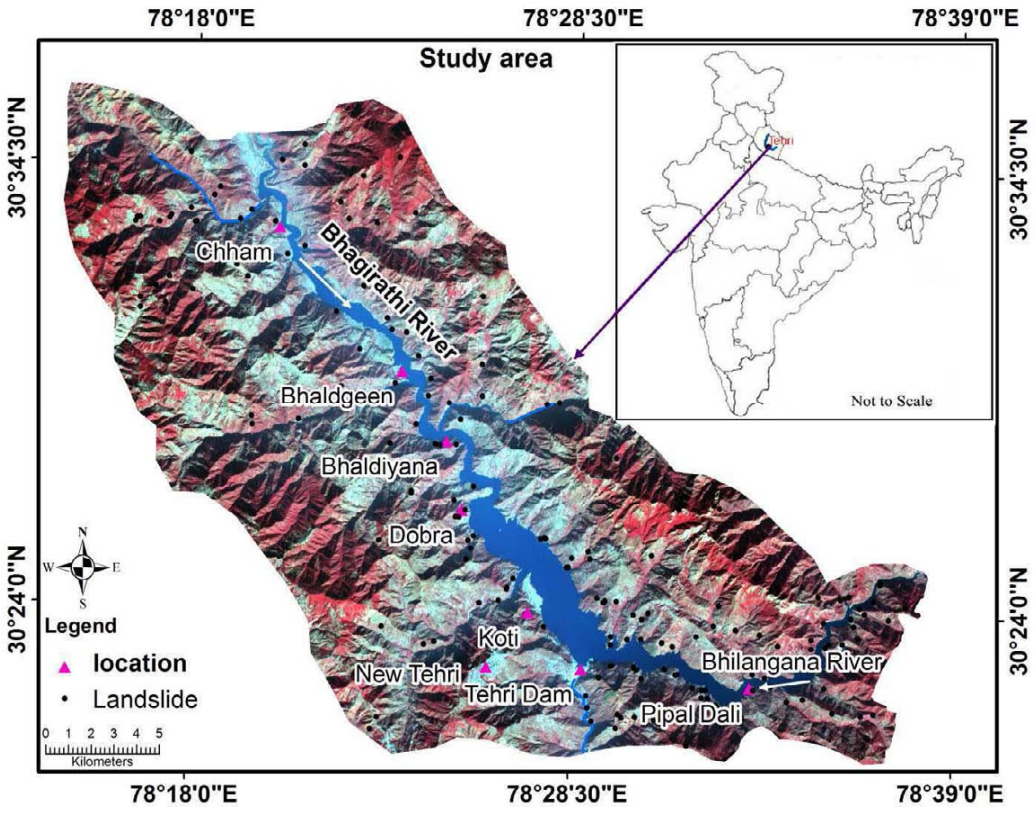

Fig.1. Location map of the study area along with landslide incidences.

Physiographically, the area is highly undulating lesser Himalayan terrain, represented by high ridges/spurs, deep valleys and abrupt/sharp slopes. In general, ridges have thick/dense to open forest on northern side while southern face is mostly covered by agricultural land. The area is a complex network of numerous streams, which are making dendritic to sub-dendritic pattern. Two major streams Bhagirathi and Bhilangana confluence at a place where a 260.5 m high Tehri dam became operational in the first decade of the century and is one of the highest rock-filled dams of the world. The construction of the dam has resulted in the formation of a huge reservoir (67 km long) in Bhagirathi and Bhilangana valley. Maximum reservoir level (MRL) is 830 m and dead storage level (DSL) is 740 m. The reservoir water fluctuates between MRL and DSL during dry and monsoon season. During the peak monsoon season, when the reservoir is at maximum level, it saturates the valley slopes. When the water level goes down, it considerably saturates the side slopes which often become unstable and may create slope instability problems in a number of places. The instability problem vary from place to place because of the following problems - (a) type of slope material, (b) Geometry of rock slope, (c) vegetation cover, and (d) human interference within the reservoir rim boundary. The drawdown condition of the reservoir has a distinctly adverse impact on the stability of the reservoir rim area, which is manifested in the form of landslides (Fig. 1). These are also called reservoir induced slope failures which are found to be varying in a range of 5m×5m to 50m×50m dimension. During field observations, it was found that these landslides gradually spread on the upper reaches of side slopes where a number of villages are situated.

Total thirteen causative factors were chosen for the susceptibility analysis of the region. Acquisition of landslide causative factors was carried out using a variety of data sources. Table 1 refers to various data used in the present study. ASTER multispectral data of VNIR (Visible Near Infra Red) range (15 m spatial resolution) and WorldView - 2 (panchromatic band) data of 0.5 m spatial resolution was used for the extraction of important factors. Raw remote sensing (ASTER) multispectral data was processed in ENVI 4.5 software. Different bands were extracted and geo-referenced according to UTM WGS 1984 Zone 44N. VNIR bands were selected for further study. WorldView -2 data was acquired in corrected form and used exclusively for landslide inventory mapping and LULC mapping.

WorldView – 2 images covered only 40% of the study area hence they were not used extensively. ASTER GDEM

(30 m spatial resolution, version -2, 2011 release) and Cartosat-1 DEM were subjected to DEM enhancement techniques such as DEM fill and sink removal for further analysis. Ancillary data such as landslide inventory, geological map, soil map and topographic maps were acquired from different sources. Processing of the ancillary data involved rasterization according to the unit grid size of 25m×25m selected for the present study. Co-registration of the remote sensing and ancillary data was carried out to prepare a base map of the study area. According to the base map thirteen terrain factor maps were prepared in the raster grid form which are discussed in this section.

Rocks of the study area belong to the following Formations – Rautgara, Mandhali, Deoban, Chandpur, Nagthat, Berinag, and Blaini. Table 2 shows the stratigraphic succession of the geological groups and formations of Tehri area. Central part of the area is represented by Chandpur Formation. Rocks of Chandpur Formation are low grade metamorphosed lustrous phyllites and highly weathered quartzites. These rocks are highly vulnerable to sliding because of the presence of well developed foliation plains and joints. Nagthat Formation is found in the western part of the study area. Rocks of Nagthat Formation are characterized by white, purple and green coloured quartzites with subordinate intercalation of grey and olive green slates with siltstones. Varying degree of weathering was observed in quartzites belonging to Nagthat Formation. Shearing was found to be common discontinuity in those rocks. In eastern part of the study area, North Almora Thrust (NAT) separates Jaunsar Group of rocks from Damtha Group (Rautgara Formation). Rocks of Rautgara Formation comprises of purple, pink and white coloured, well jointed, medium grained quartzites, minor slates and metavolcanics. Deoban Formation is found in eastern and north-eastern part of the study area. It is sandwiched between Rautgara Formation and Berinag Formation in the southern part of the study area. Deoban Formation consists of fine grained dolomitic limestone with minor phyllitic intercalations. These rocks are mainly found at the higher ridges. Rocks of Berinag Formations are exposed in the eastern part of the area. It is separated by Berinag thrust at its base. These rocks are mostly quartzites. Bliani Formations are found in the western part of the study area. This Formation comprises of quartzites, slates and carbonate rocks. Two major synclines and NAT are present in the area.

A geological map was prepared following the work of Valdiya (1980) and field observations (Fig. 2a). A regional soil map was prepared on the basis of the published report of Watershed Management Directorate, Dehradun. Following three categories: alluvial sandy loam, sandy loam and forest/black soil are represented in the area (Fig. 2b). Remote sensing data was used to acquire landslide inventory, LULC and photo-lineament by applying digital image processing techniques such as NDVI, supervised classification, band rationing etc. Onscreen visualization based on colour, tone, texture, pattern, shape and shadow was also performed for identification of LULC boundary and photo-lineament (Gupta et al. 1999). Five categories of LULC namely: dense forest, open/scrub forest, agricultural land, settlement/barren land and water body were derived from combination of topographic map and satellite imageries (Fig. 2c). ASTER GDEM was used for the extraction of topographic attributes namely slope, aspect, relative relief, profile curvature, topographic wetness index (TWI) and stream power index (SPI). Aspect is also an important factor considered in LSM (Nagrajan et al. 1998; Saha et al. 2002; Kanungo et al. 2009a). Aspect is the direction a slope faces with respect to north. Aspect determines the effect of solar heating, soil moisture, and dryness of air (Dai et al. 2001; Suzen and Doyuran 2004; Yalcin 2008). Aspect map of the area was prepared on the basis of DEM manifesting nine classes namely, flat (-1), north (0° – 22.5° and 337.5°-360°), northeast (22.5°-67.5°), east (67.5°-112.5°), southeast (112.5°-157.5°), south (157.5°-202.5°), southwest (202.5°-247.5°), west (247.5°-292.5°) and northwest (292.5°-337.5°) (Fig. 2d). Literature review suggested that slope angle substantially impact the landslides (Kanungo et al. 2006; Gupta et al. 2008; Dahal et al. 2009; Kayastha et al. 2013). Slope map was prepared covering five classes: very low/flat (0° -10°), low (10°-20°), moderate (20° -32°), high (32°-45°) and very high (>45°) (Fig. 2e). Relative relief is the difference between maximum and minimum elevation

Table 1. Stratigraphic succession and rock type represented in study area (Valdiya, 1980)

Group	Inner Lesser Himalaya Formations	Outer Lesser Himalaya	Age	Rock type
Mussoorie		Blaini	Neoproterozoic	Quartzite, limestone, slates, phyllites and conglomerate
Jaunsar	Berinag	Nagthat	Mesoproterozoic	Weathered quartzite intercalated with slate
		Chandpur	Mesoproterozoic	Low grade lustrous phyllites
Tejam	Deoban	Mandhali	Mesoproterozoic	Dolomitic limestone with phyllitic intercalations
Damtha	Rautgara		Mesoproterozoic (>1300my)	Quartzite, slate, metavolcanic rocks

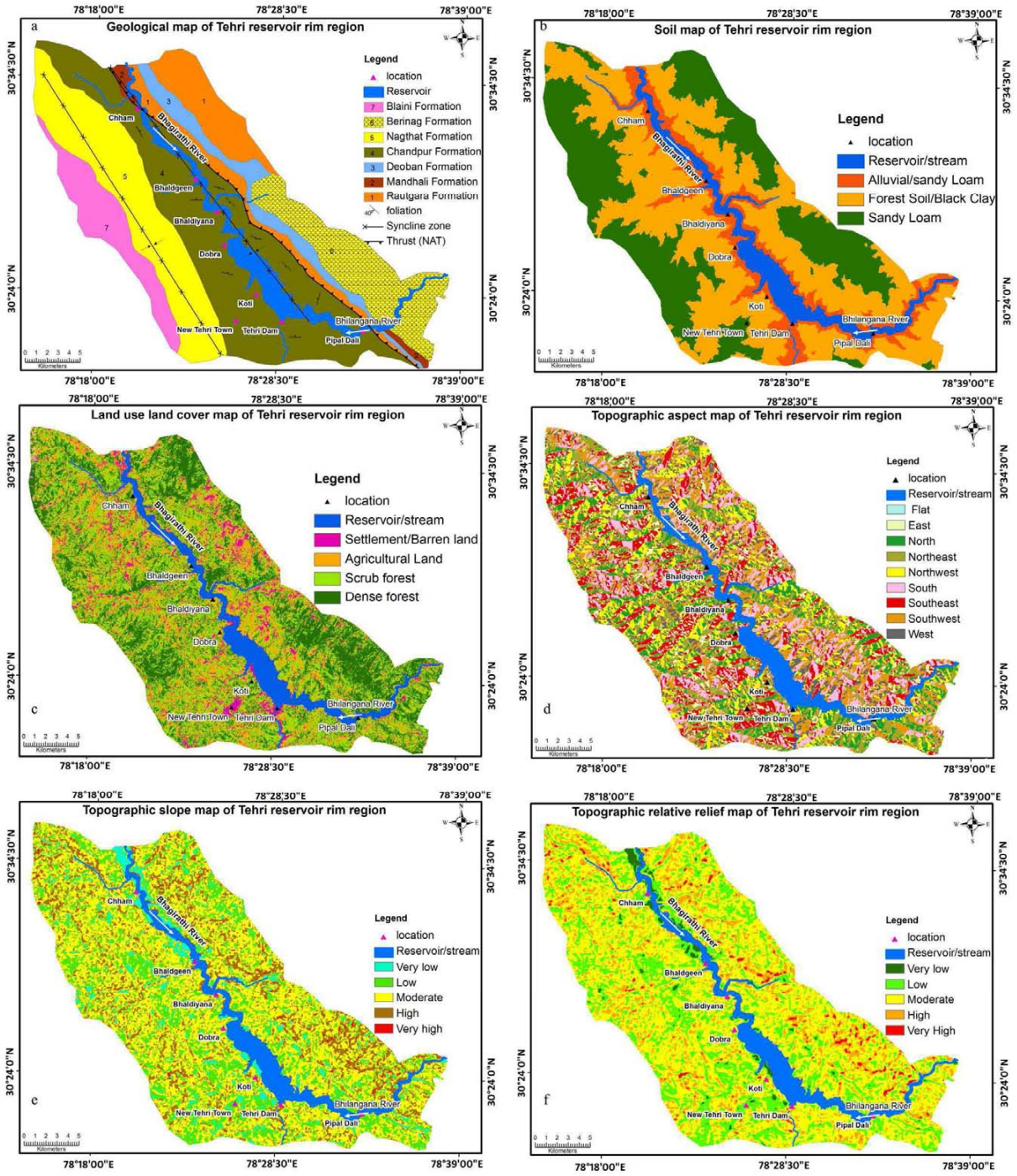

Fig.2. Factors used to identify the landslide susceptible areas in the present study, **(a)** Geology, **(b)** soil, **(c)** LULC, **(d)** aspect, **(e)** slope, **(f)** relative relief.

point within a facet or area and it is widely used in susceptibility model (Gupta et al. 1999; Saha et al. 2005; Kanungo et al. 2009a). In the present study, relative relief was found to be varying between 0 to 367 m.

Following five classes of relative relief: very low relief (0–30 m), low relief (30 m–60 m), moderate relief (60 m–100 m), high relief (100 m–150 m) and very high relief (>150 m) were considered for landslide susceptibility study (Fig. 2f). Together with other factors, curvatures control the flow of water in and out of slopes and are, therefore important in the study of landslides (Ayalew et al. 2004; Dahal et al. 2009). Profile curvature was considered for this study. Accordingly, a profile curvature map was prepared showing concave and convex profile.

Table 2. Data used in present study

Data Type	Sensor	Resolution/ Scale	Data Derivative
Image	ASTER	15 m	LULC
	WorldView - 2		Photo-lineament
		0.5 m	Landslide inventory
DEM	Cartosat 1	2.5 m	Slope
	DEMASTER GDEM	30 m	Aspect
			Relative relief Profile curvature TWISPI
			Drainage
Ancillary	Geology map	1:250000	Vector geology map
		1:250000	Vector soil map
		1:25000	Vector topographic map
		1:25000	Vector Landslide Inventory

Two secondary topographic factors, TWI and SPI, which were hardly employed in landslide susceptibility study in Uttarakhand Himalayan region, were used as an input in this model. TWI considers catchment area and slope gradient. It can be calculated using formula:

$$TWI = \ln \frac{CA}{\tan slp} \quad (1)$$

in which CA stands for catchment area and *slp* for slope gradient. TWI is associated with flow accumulation at the given terrain. It is effectively used to understand the soil moisture condition and other related phenomenon (Wilson and Gallant 2000; Wilson 2011). TWI was computed in Arc GIS 10.1 software. Resulting value of TWI and SPI were represented on natural log scale. Range of TWI was found between 5–19. TWI map was classified into four classes (Fig. 3a). Another important parameter SPI was calculated using formula given below

$$SPI = \ln (CA \times \tan slp) \quad (2)$$

SPI represents the erosive power of the streams in a terrain (Wilson and Gallant, 2000). SPI was found to range between 1.5 to 15. Five classes of SPI were achieved using natural break classifier (Fig. 3b).

The rugged terrain of Himalaya is prone to drainage induced landslides (Gupta et al. 1999, Saha *et al.* 2002; *Saha et al.* 2005). Drainage buffer map was prepared containing 0–50 m, 50–100 m, 100–150 m, 150–200 m and > 200 m distances (Fig. 3c). Distance to lineament is a fair measure of the prediction of landslide occurrence and considered as indispensible input in susceptibility model by a number of authors (Gupta *et al.* 1999; Saha *et al.* 2005; Dahal *et al.* 2008; Pradhan et al. 2010). Photo lineament layer was prepared using edge detection method on DEM and calibrated by onscreen visualization process. Complying with field observations, a photo-lineament buffer map was prepared covering 0–50 m, 50–100 m, 100–150 m, 150–200 m and >200m distances (Fig. 3d). Field observations provided insight about frequency of landslides along the reservoir rim region, accordingly, reservoir multi-buffer map (100 m, 200 m, 300 m, 400 m, 500 m) was prepared (Fig. 3f). Following the previous logic a road buffer map was prepared showing 0–50 m, 50–100 m, 100–150 m, 150–200 m and >200m distances (Fig. 3e). External factors such as rainfall, earthquake and temperature variation were not used in this model because of their temporal nature (Gupta *et al.* 2008). Most of the landslides are triggered in the monsoon period (<5% triggered during other seasons) and the precipitation is uniformly distributed throughout the region; hence the temporal factor rainfall, was not considered in the present landslide susceptibility study.

METHODOLOGY

Procedure of LSM in the present region was initiated by collecting landslide information. A landslide inventory map was prepared using historical information available, field observation/GCP collection and satellite data. With the help of local population and remote sensing data a point vector map of landslide inventory was created in GIS domain. Dimensions of landslides were varying between 25 m^2 to 2500 m^2. Most of the landslides were found to be shallow in nature. A total of 195 landslide occasions were covered in the form of point vector (Fig. 1).

One important aspect was the use of factors in GIS based model. But in a GIS-based study, it is also necessary to be sure that any selected factor is operational (has a certain degree of affinity with landslides), complete (is fairly represented all over the study area), no uniform (varies spatially), measurable (can be expressed by nominal, ordinal, interval, ratio scales), and non-redundant (its effect should not account for double consequences in the final result) (Yalcin 2008). More or less each factor was found to be fit according to the above mentioned criteria.

The present study is based on the use of AHP method for synthesising weights of the factors/classes. Application of AHP method is widely used in site selection, suitability analysis and LSM (Ayalew et al. 2005; Yalcin 2008; Feizizadeh and Blaschke 2012). AHP is a multi criterion decision making technique introduced by Saaty (1980) which allows subjective as well as objective factors to be considered in the decision-making process (Yalcin 2008; Feizizadeh and Blaschke 2012). It is based on three principles: decomposition, comparative judgment and synthesis of priorities (Malczewski, 1999; Yalcin 2008; Kayastha et al. 2013). AHP breaks complex decision making

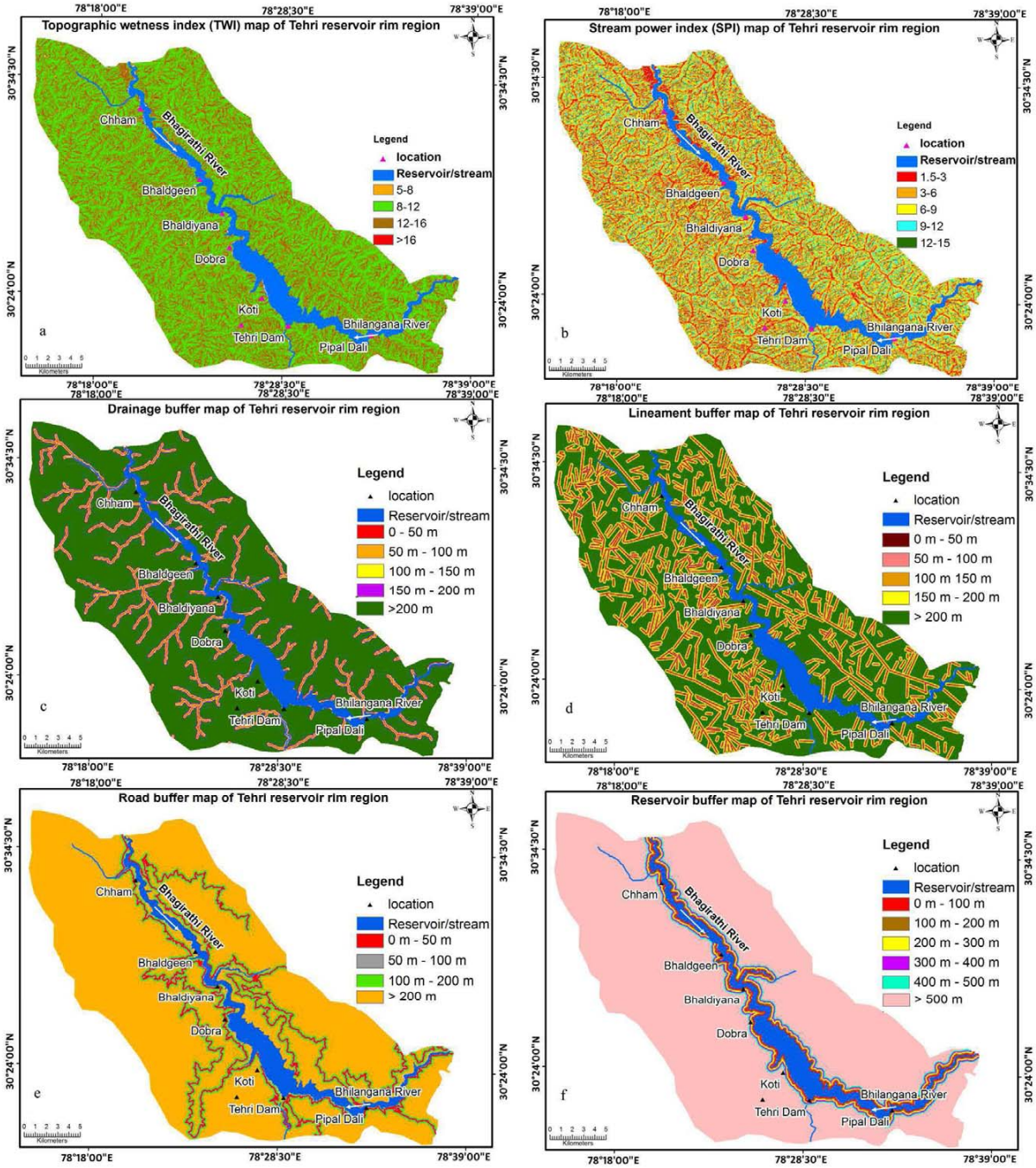

Fig3. Factors used to identify landslide susceptible areas in the present study **(a)** TWI, **(b)** SPI, **(c)** drainage buffer, **(d)** photo-lineament buffer, **(e)** road buffer, **(f)** reservoir buffer

problem into a hierarchy of factors and alternatives. Factors and alternatives are assigned weights on a nine point ordinal scale (Table 3) by virtue of pair-wise comparison between them. Factors or their classes are arranged in the form of matrix which contains equal number of rows and columns, where scores are recorded on one side of the diagonal, while values of 1 are placed in the diagonal of the matrix (Satty 1977; Gorsevski et al. 2006). Pair-wise comparison and judgment of score is influence by professional knowledge. Source of knowledge of landslide causative factors can be subjective or it may be perceived from objective approach. Yalcin (2008) emphasized that subjective as well as objective factors to be considered in decision making process. In this study relative value of each pair of the factors/classes was determined on the basis of professional knowledge from the field work and presence of landslide in those classes.

When the factor on the vertical axis is more important than the factor on the horizontal axis, this value varies between 1 and 9 and conversely, the value varies between the reciprocals 1/2 and 1/9 (Saaty 1980; Yalcin 2008). Matrix calculation gives factor/class weights in terms of eigenvector. Calculation of maximum eigenvalue is also a part of the AHP model. Subjective decision rule can violate the transitivity rule and thus cause an inconsistency (Feizizadeh and Blaschke 2012). One of the important aspects of the AHP principle is the calculation of consistency index (CI) and consistency ratio (CR). Saaty (1980) formulated consistency index as:

$$CI = \frac{\lambda_{max} - N}{(N-1)} \quad (3)$$

where λ_{max} is the maximum eigenvalue and N is the number of elements present in the row/column of the matrix. CR can be calculated by ratio CI/RI, where RI stands for random index (Satty 1980). Random index (Table 4) was compiled by Satty (1980) on the basis of a number of random samples. CR value of 0.1 is the maximum threshold of consistency of the matrix. CR value >0.1 is thought to be inconsistent where as value 0 indicates perfectly consistent comparison result. Table 5 refers to AHP based matrix for the factors/ classes showing scores awarded on ordinal scale, eigenvector, CR and maximum eigenvalue.

AHP method has its advantages in weighting/rating of factors and their classes along with some deficiencies. Relative scoring of the factors largely bank on the knowledge of a person or professional. Relative preference given to a factor by a person or professional is often not recognised by others, which is a major drawback of any subjective decision making system. Nonetheless, pair-wise comparison provides a simple and acceptable decision rule. In landslide studies, some factors have certain degree of dependency in influencing landslides whereas AHP considers factors in hierarchy as an independent entity. For example a relatively moderate slope can fail owing to increase in the moisture content of the slope forming material (TWI and SPI parameters) but in AHP system, moderate slope will be given lesser preference compared to high slope category. Overall AHP multi criteria decision making provides a very flexible and simple decision making which can be conveniently accommodated in the GIS domain.

Table 3. Ordinal scale represents preference of judgement (Saaty 1977)

Preference/ ordinal scale	Degree of preference	Remarks
1	Equally	Factors inherit equal contribution
3	Moderately	One factor moderately favoured over other
5	Strongly	Judgement strongly favour one over other
7	Very strongly	One factor very strongly favoured over other
9	Extremely	One factor favoured over other in highest degree
2,4,6,8	Intermediate	Compensation between weights 1,3,5,7 and 9
Reciprocals	Opposite	Refers inverse comparison

Table 4. Random consistency index (RI) (Saaty, 1980)

N	1	2	3	4	5	6	7	8	9	10	11	12	13	14	15
RI	0	0	0.58	0.9	1.12	1.24	1.32	1.41	1.45	1.49	1.51	1.53	1.56	1.57	1.59

Next step was calculation of landslide susceptibility index (LSI). It was computed using weighted arithmetic sum method which can be formulated as given below:

$$LSI = \sum_{J=1}^{N} \text{Weigth of factor } (W_j) \text{ x weight of factor classes } (W_{ij}) \quad (4)$$

where W_{iJ} denotes weight of *ith* class of factor J. LSI map was classified into very low, low, moderate, high and very high susceptibility classes employing natural break (ESRI 2012) classification method.

RESULTS

LSM was performed using AHP method. AHP was used to weight factors and their classes (Table 5). Raster maps of each factor were assigned weight values on cell by cell basis. Integration of weighted raster maps was performed using eq. 4. Integration resulted in a LSI map which contained numerical susceptibility information in which higher LSI values indicate high susceptibility and lower value indicate low susceptibility (Fig.4). LSI values are found in a range of 8.58 to 53.89 (Fig. 4). Natural break classifier was used to calculate class break values of the continuous LSI map, which is depicted in Fig. 5 and accordingly LSI map is classified into the following five categories: Very low susceptibility, low susceptibility, moderate susceptibility, high susceptibility and very high susceptibility (Fig. 6). 23% of the entire area is found in very low susceptibility class, 34% in low susceptibility class, 25% in moderate susceptibility class, 15% in high susceptibility class and 3% in very high susceptibility (Fig. 7). Results have indicated that areas immediate to the reservoir banks mostly fall in high susceptibility classes. Result have also reflected that high susceptible classes occupied areas around the drainage network. Low susceptibility classes are observed in areas having flatter terrain, dense forest cover and sparse forest cover. Settlement areas have been observed in moderate to high susceptibility classes.

VALIDATION

Validation was performed to obtain the accuracy of

Table 5. Refers AHP scores of factors/classes, eigenvector, CR and Maximum eigenvalue

Factors and Classes	1	2	3	4	5	6	7	8	9	10	11	12	13	Normalized Eigen (Weight)
Factors comparison														
Geology (1)	1													0.0342
Soil (2)	1/3	1						0.076						
LULC (3)	½	1	1											0.126
Lineament (4)	3	4	4	1										0.131
Drainage (5)	4	4	4	3	1									0.021
Slope (6)	4	4	5	3	1	1								0.077
Aspect (7)	¼	1/3	1/3	1/3	¼	1/5	1							0.065
Relative relief (8)	3	4	4	2	1/3	1/3	3	1						0.023
TWI (9)	½	1	2	1/3	¼	¼	2	1/3	1					0.21
SPI (10)	1/3	½	½	¼	1/5	1/5	2	¼	1/3	1				0.0175
Reservoir Buffer (11)	4	4	5	4	3	3	5	4	5	5	1			0.127
Curvature (12)	¼	1/3	¼	1/5	1/5	1/6	½	1/3	¼	½	1/5	1		0.0342
Road Buffer (13)	4	4	4	3	1	1	5	3	4	5	1/3	5	1	0.076
CR = 0.067, Maximum eigenvalue – 14.2														
Factor classes comparison														
Geology														
Blaini Formation (1)	1													0.066
Nagthat Formation (2)	4	1												0.26
Chandpur Formation (3)	5	2	1											0.345
Berinag Formation (4)	1	¼	1/5	1										0.068
Deoban Formation (6)	1	¼	1/5	1	1									0.063
Mandhali Formation (7)	1/3	1/5	1/5	1/3	½	1								0.038
Rautgara Formation (8)	4	1/3	1/3	3	3	4	1							0.160
CR = 0.0472, Maximum eigenvalue = 8.331														
Soil Cover														
Alluvial/sandy Loam (1)	1													0.636
Forest Soil/Black Clay (2)	1/5	1												0.104
Sandy Loam (3)	1/3	3	1											0.258
CR = 0.0192, Maximum eigenvalue = 3.03														
Relative relief														
Very low (1)	1													0.045
Low (2)	2	1												0.062
Moderate (3)	3	3	1											0.119
High (4)	5	5	3	1										0.242
Very high (5)	8	7	5	4	1									0.529
CR = 0.068, Maximum eigenvalue = 5.27														
Slope category														
0°-10° (1)	1													0.039
10°-20° (2)	2	1												0.057
20°-32° (3)	4	3	1											0.122
32°-45° (4)	6	5	3	1										0.241
>45° (5)	8	7	5	4	1									0.539
CR = 0.0619, Maximum eigenvalue = 5.24														
Lineament Buffer														
0 – 50m (1)	1													0.418539
50 – 100m (2)	½	1						0.262518						
100m – 150m (3)	1/3	½	1											0.159923
150m – 200m (4)	¼	1/3	½	1										0.0972536
>200m (5)	1/5	¼	1/3	½	1									0.0617666
Consistency Ratio = 0.017, Maximum Eigenvalue = 5.068														
Drainage Buffer														
0 – 50m (1)	1													0.479
50 – 100m (2)	1/3	1												0.267
100m – 150m (3)	¼	1/3	1											0.128
150m – 200m (4)	1/5	¼	½	1										0.083
>200m (5)	1/7	1/6	¼	1/3	1									0.041
CR = 0.051, Maximum eigenvalue = 5.207														
Land use/ Land cover														
Dense forest (1)	1													0.069
Sparse forest (2)	3	1												0.149
Agricultural land (3)	4	2	1											0.243
Settlement /Fallow Land (4)	5	4	3	1										0.537
CR = 0.039, Maximum eigenvalue = 4.11														

Table 5. Contd...

Factors and Classes	1	2	3	4	5	6	7	8	9	10	11	12	13	Normalized Eigen (Weight)
Aspect														
North (1)	1													0.0406
Northwest (2)	3	1												0.0625
West (3)	3	2	1			0.083								
Southwest (4)	4	3	3	1										0.149
South (5)	5	4	4	3	1									0.295
Southeast (6)	4	3	3	3	1/3	1								0.204
East (7)	2	2	1	1/3	¼	1/3	1							0.0791
Northeast (8)	2	1	½	1/3	¼	¼	½	1						0.0565
Flat (9)	1/3	1/3	1/3	¼	1/5	1/5	1/3	1/3	1					0.0284
CR = 0.0738, Maximum eigenvalue = 9.59														
TWI														
5-8 (1)	1				0.068									
8-12 (2)	3	1												0.134
12-16 (3)	4	3	1											0.268
16-19 (4)	5	4	3	1										0.52
5-8 (1)	1	1/3	1/4	1/5	1									0.068
CR = 0.060, Maximum eigenvalue = 4.18														
SPI														
1.5-3 (1)	1													0.060
3-6 (2)	2	1												0.094
6-9 (3)	3	2	1											0.155
9-12 (4)	4	3	2	1										0.238
12-15 (5)	5	4	3	2	1									0.451
CR = 0.0317, Maximum eigenvalue = 5.12														
Curvature														
Concave	1													0.66
Convex	1/2	1						0.33						
CR = 0.0, Maximum eigenvalue = 2														
Road Buffer														
0 – 50	1													0.558
50 – 100	1/3	1												0.255
100 - 200	1/5	1/3	1											0.122
>200	1/6	¼	1/3	1										0.062
CR = 0.049, Maximum eigenvalue = 4.14														
Reservoir buffer														
0 -100 (1)	1													0.448
100 – 200 (2)	1/3	1												0.220
200 – 300 (3)	1/4	1/2	1											0.142
300 – 400 (4)	1/5	1/3	½	1										0.090
400 – 500 (5)	1/6	¼	1/3	½	1	2								0.058
>500 (6)	1/7	1/5	¼	1/3	½	1								0.03
CR = 0.0325, Maximum eigenvalue = 6.16														

landslide susceptibility map. Accuracy of landslide susceptibility map is the capability of a map to delineate landslide free and landslide susceptible areas. Comparison of different models and model parameter variables can also be performed from validation (Begueria, 2006). Accuracy and objectivity depend on model accuracy, input data, experience of professionals and size of the study area (Soeters and van Westen, 1996). There are several statistical methods available for analyzing model accuracy such as error rate, ROC (Receiver Operating Characteristics) plot, success rate curve and prediction rate curve. Error rate and ROC curve method depend upon wrongly classified present landslide areas (False positives) and wrongly classified non-landslide areas (False negatives) whereas prediction rate curve technique depend upon training and testing landslide data. These methods exclusively depends upon the training data. In the present study, cumulative percentage curve/ success rate curve technique, which considers existing landslide, was used to validate the accuracy of the landslide susceptibility map. Success rate curves were achieved by plotting cumulative percent of LSI in descending order against cumulative percent of landslide on X and Y axis respectively. Fig. 8 is a cumulative percentage curve of the presented model. It indicates that 58% of landslides fall under 100 - 90% of high susceptible classes whereas 22% of the landslides fall under 90-70% of high susceptible class, and accordingly other values follow. Hence, percentage cumulative curve clearly states the accuracy of the landslide susceptibility map. Further, Area under curve (AUC) value of accuracy curve was calculated by simple trapezium

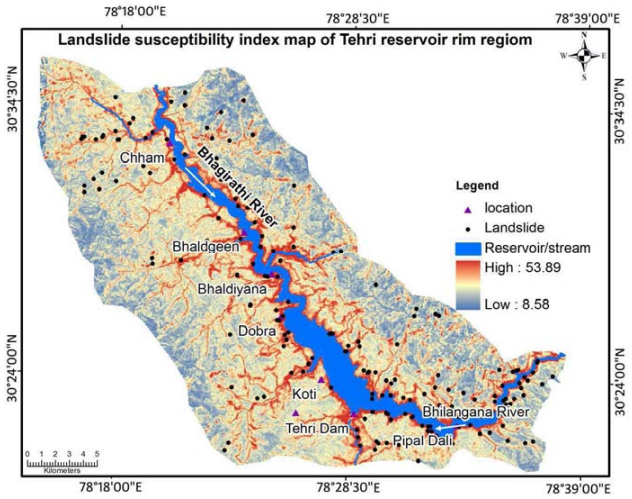

Fig.4. Landslide susceptibility (LSI) map of the Tehri reservoir rim area.

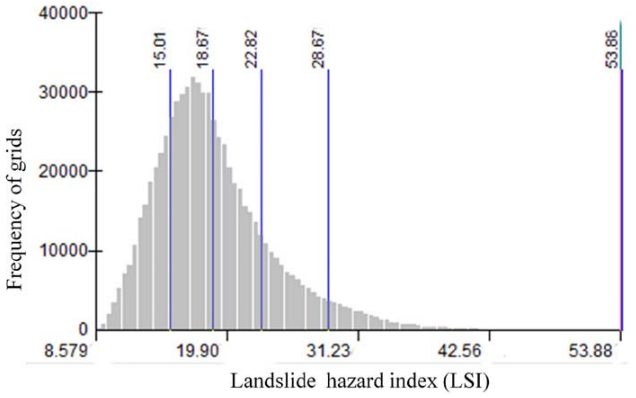

Fig.5. Threshold values chosen for classification of LSI map

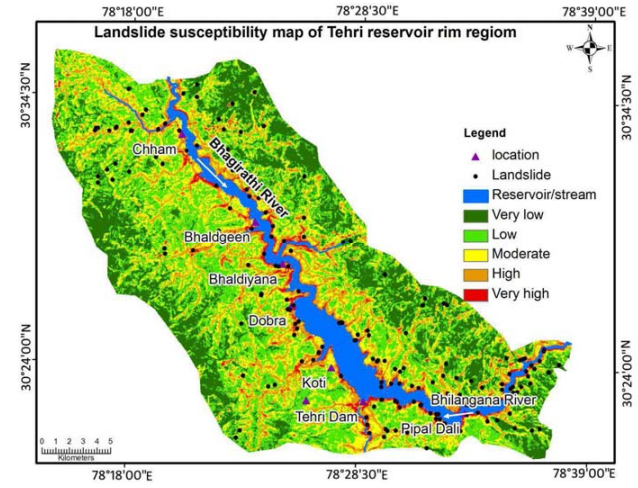

Fig.6. Landslide susceptibility map of the Tehri reservoir rim area

method. AUC value 0.787 is achieved for the present model which can be converted in teams of percent success rate accuracy of 78.7%. So it can be said that model gave an accuracy of 78.7%. Nonetheless, landslide density of the

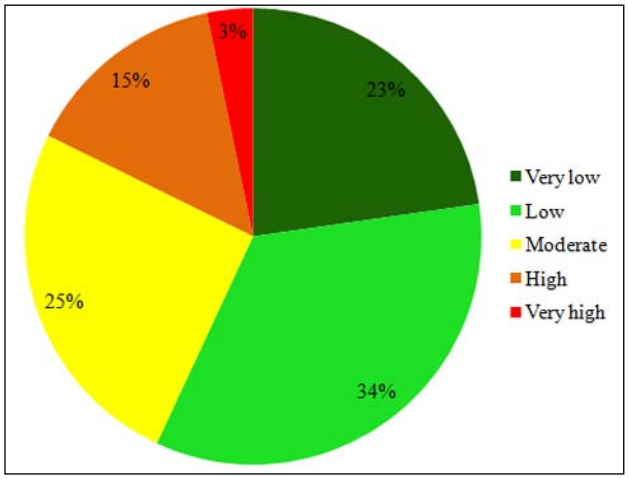

Fig.7. Pie chart showing density of landslide susceptible classes

susceptible classes leads to the assessment of the overall quality of the landslide susceptibility map (Sarkar and Kanungo 2004; Kayastha *et al.* 2012). Table 6 depicts the landslide density values in which it is noticeable that the landslide density for the very high susceptible class is 2.147, which is markedly larger than the other susceptible classes. It can also be observed from the Table 6 that there is a continuing decrease in the landslide density values from the very high to low susceptible classes. On the basis of landslide density results, it can be said that the computed susceptibility classes largely comply with the field conditions (Fig. 9 and Fig. 10). Fig. 9 (A-D) are the landslides observed along the side slopes adjoining the reservoir which has been reflected in the susceptibility map as high to very high susceptibility classes (Fig. 6) where as Fig.9 (E-F) shows the landslides

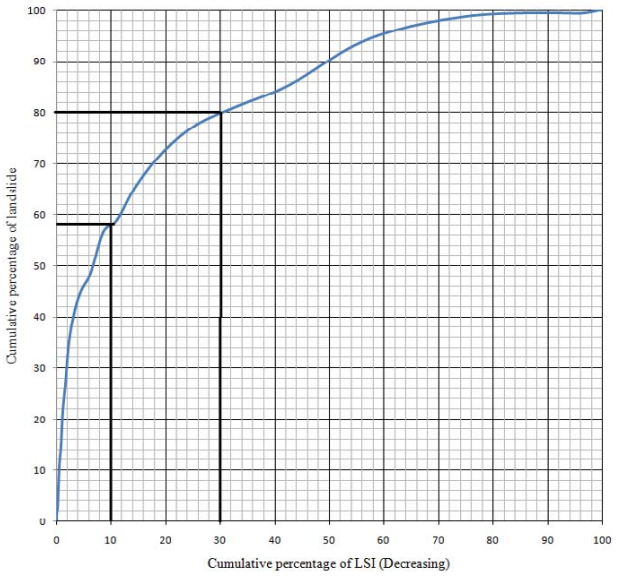

Fig.8. Cumulative percentage curve LSI

Fig.9. A,B,C and **D** refers to the landslide incidences along the side slopes adjoining the reservoir where as **E** and **F** shows the landslides incidences on the steep cut slopes along the road.

adjoining the road (least distance to road) network and are also manifested in terms of high and very high susceptibility classes in the LSM. Fig. 10A depicts a landslide observed along a stream and this kind of terrain is reflected as high and very high susceptibility class in the susceptibility map. Fig 10B and 10C shows landslides in phyllitic rocks and steep slopes respectively and are also reflected in susceptibility map as higher susceptibility classes.

Table 6. Landslide density in different classes of landslide susceptibility map

Susceptibility classes	Area (km^2)	Landslide frequency (No.)	Landslide frequency density
Very low	5	0	0.000
Low	80	5	0.062
Moderate	206	13	0.063
High	198	46	0.232
Very High	61	131	2.147

CONCLUSIONS

The present paper provides insights into the capability of multi-criteria decision making system AHP in predicting landslide susceptible areas. AHP method was successfully

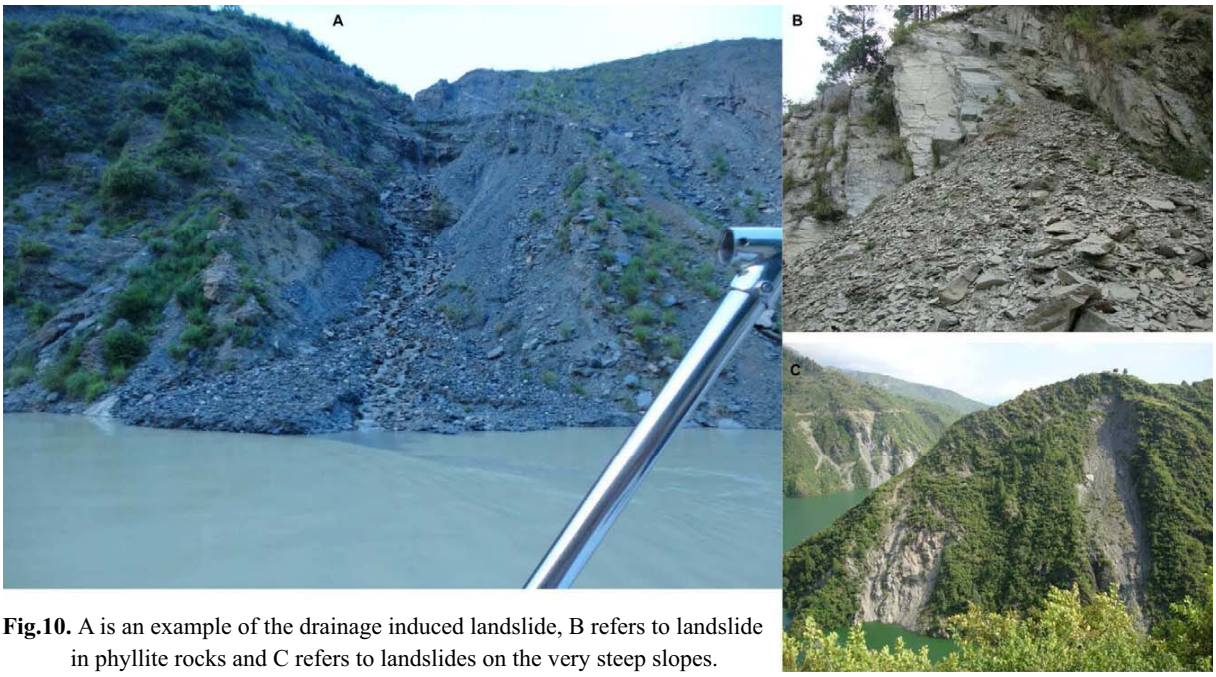

Fig.10. A is an example of the drainage induced landslide, B refers to landslide in phyllite rocks and C refers to landslides on the very steep slopes.

used to assign weights to factors and their classes. Judgement in the pair-wise comparison matrix was motivated by the present landslides in the area. Landslide susceptibility map provided critical evaluation of the factor classes present in the area. Among the slope classes, most of the high susceptible area is observed in very high and high slope angle classes. Generally, in a terrain having high slope angle, the weight of the possible mobilized material under gravity will be more as compared to a moderate slope angle. Shear strength being same in both the cases, a steep slope with more mobilizing force may fail early. High susceptible area is observed in high and very high relative relief classes. High relative reliefs are surface manifestation of cliffs and ridges, which are often rendered unstable by the influence of triggering factors such as rainfall and earthquakes. Southern aspect of the study area, which is receiving excessive sun radiation and high rainfall, are observed under higher susceptibility classes. Incidentally, a number of agricultural terraces are present on the southwest facing slopes leading to more instability. Among the secondary topographic parameters, higher susceptibility classes are observed in the higher TWI and SPI ranges. Higher TWI ranges are associated with the increasing water infiltration which often leads to increase in the pore water pressure and further reduces the soil strength, hence making the terrain prone to slope failures. SPI indicates the erosive power of the streams and lower ranges of SPI is related to the low erosive power of the streams. High susceptibility classes are also observed in the areas in closer proximity to drainages (drainage buffer) and it can be attributed to the stream bank erosion due to the river flow such as gulling, toe cutting which further leads to landslides.

Lithology of the area belongs to different formations and is represented by characteristic rock type, which might govern landslide incidence. High susceptibility classes were observed in the rocks belonging to Chandpur and Nagthat Formation where low susceptibility classes were observed in rocks belonging to Blaini, Mandhali, and Deoban Formations. Rocks belonging to Chandpur Formation are mostly weathered phyllites which are inherently failure prone. Rocks of Blaini, Mandhali, and Deoban Formations constituted of slate, quartzite, siltstone and carbonate rocks and are found in low susceptibility classes. Alluvial soil has been observed at lower elevations along the drainage network and are not well compacted and it leads to slope failures which is manifested in the form of high susceptible area in the landslide susceptibility map. High susceptible area was observed all around the fringes of the reservoir rim owing mainly to the process of reservoir side slope settlement process. Road network and other infrastructures were observed along the reservoir rim boundary. Higher susceptibility classes were observed all along the areas in closer proximity to road. Impact of lineament and slope profile curvature do not show any characteristic pattern as observed from the landslide susceptibility map. Combined effects of unplanned construction and reservoir side slope adjustment process results in a number of landslides during monsoon season

which is reflected in the susceptibility map. Forest areas were observed in low susceptibility region of the map. Validation was performed using cumulative percentage/ success rate curve technique and gave an acceptable success rate accuracy of 78.7%. Landslide density frequency results have also found to be matching with the existing field conditions.

LSM studies of the Tehri reservoir rim region can lead to the identification of vulnerable valley slopes of the reservoir which can be further studied analytically. Impact of the reservoir impoundment on the susceptible side slopes can open a whole new dimension of research such as hydrogeological changes in the side slopes, changes in the discontinuity orientation, and sinking of side slopes etc. A detailed analytical (deterministic) approach based on geotechnical properties of the susceptible slopes would be a better way to understand the process of reservoir induced side slope failure and consequently mitigation measures can be adopted by the planners.

Acknowledgements: We would like to acknowledge THDC India Limited, Rishikesh, Uttarakhand for all their support during field investigations. We would also like to acknowledge Department of Earth Sciences IIT Roorkee, Roorkee, Uttarakhand for providing important data and software used in this study.

References

Aleotti, P. and Chowdhury, R. (1999) Landslide hazard assessment: summary review and new perspectives. Bull. Engg. Geol. Environ., v.58, pp.21–44.

Anbalagan, R. (1992) Landslide hazard evaluation and zonation mapping in mountainous terrain. Engg. Geol., v.32, pp.269–277.

Anbalagan, R., Chakraborty, D. and Kohli, A. (2008) Landslide hazard zonation (LHZ) mapping on meso-scale for systematic town planning in mountainous terrain. Jour. Sci. Indus. Rese., v.67, pp.486–497.

Arora, M.K., Das Gupta, A.S. and Gupta, R.P. (2004) An artificial neural network approach for landslide hazard zonation in the Bhagirathi (Ganga) Valley, Himalayas. Int. Jour. Remote Sens., v.25, pp. 559–572.

Ayalew, L., Yamagishi, H. and Ugawa, N. (2004) Landslide susceptibility mapping using GIS-based weighted linear combination, the case in Tsugawa area of Agano River, Niigata Prefecture, Japan. Landslides, v.1, pp.73–81

Ayalew, L., Yamagishi, H., Marui, H. and Kanno, T. (2005) Landslides in Sado Island of Japan: Part II. GIS-based susceptibility mapping with comparisons of results from two methods and verifications. Engg. Geol., v.81, pp.432–445.

Brabb, E.E. (1984) Innovative approaches to landslide hazard mapping. *In:* Proc. 4th Internat. Symposium on Landslides, Toronto, v.1, pp.307–324.

Begueria, S. (2006) Validation and evaluation of predictive models in hazard assessment and risk management, Nat. Hazard., v.37(3), pp. 315-329.

Chakraborty, D. and Anbalagan, R. (2008) Landslide hazard evaluation of road cut slopes along Uttarkashi – Bhatwari road, Uttaranchal Himalaya. Jour. Geol. Soc. India, v.71, pp. 115-124.

Champatiray, P.K., Suvarna, D., Lakhera, R.C. and Sati, S. (2007) Fuzzy based method for landslide hazard zonation in active seismic zone of Himalaya. Landslides, v.5, pp.101–111.

Chung, C.J. and Fabbri, A.G. (2003) Validation of spatial prediction models for landslide hazard mapping. Nat Hazard., v.30, pp.451–472.

Dahal, R. K., Hasegawa, S., Nonomura, A., Yamanaka, M., Dhakal, S. and Paudyal, P. (2008) Predictive modelling of rainfall-induced landslide hazard in the Lesser Himalaya of Nepal based on weights-of-evidence. Geomorphology, v.102, pp.496-510.

Dahal, R. K., Hasegawa, S., Nonomura, S., Yamanaka, M., Masuda, T. and Nishino, K. (2009) GIS-based weights-of-evidence modelling of rainfall-induced landslides in small catchments for landslide susceptibility mapping. Environ. Geol., v.54, pp. 314–324.

Dai, F.C., Lee, C.F., Li, J. and Xu, Z.W. (2001) Assessment of landslide susceptibility on the natural terrain of Lantau Island, Hong Kong. Environ. Geol., v.40, pp.381–391.

Dai, F.C., Lee, C.F. and Ngai, Y.Y. (2002) Landslide risk assessment and management: an overview. Engg. Geol., v.64(1), pp.65–87.

Das, I., Sahoo, S., van Westen, C. J., Stein, A. and Hack, R. (2010) Landslide susceptibility assessment using logistic regression and its comparison with a rock mass classification system, along a road section in the northern Himalayas (India). Geomorphology, v.114, pp.627–637.

Das, I., Stein, A., Kerle, N. and Dadhwal (2012) Landslide susceptibility mapping along road corridors in the Indian Himalayas using Bayesian logistic regression models. Geomorphology, v.179, pp. 116-125.

Ercanoglu, M. and Gokceoglu, C. (2004) Use of fuzzy relations to produce landslide susceptibility map of a landslide prone area (West Black Sea Region, Turkey). Engg. Geol., v.75 (3–4), pp.229–250.

ESRI. FAQ. (2012) What is the Jenks optimization method? http:/ /support.esri.com/en/ knowledgebase/techarticles/detail/ 26442.

Feizizadeh, B. and Blaschke, T. (2103) GIS-multicriteria decision analysis for landslide susceptibility mapping: comparing three methods for the Urmia lake basin, Iran, Nat Hazards, v.65, pp.2105–2128

Fell, R., Corominas, J., Bonnard, C., Cascini, L., Leroi, E. and Savage, W.Z. (2008) Guidelines for landslide susceptibility,

hazard and risk zoning for land-use planning. Engg. Geol., v.102 (3–4), pp.99–111.

Ghosh, S., Carranza, E. J. M., van Westen, C. J., Jetten, V. and Bhattacharya, D. N. (2011) Selecting and weighting spatial predictors for empirical modeling of landslide susceptibility in the Darjeeling Himalayas (India). Geomorphology, v.131, pp.35-56.

Gorsevski, P.V., Jankowski, P. and Gessler, P.E. (2006) An heuristic approach for mapping landslide hazard by integrating fuzzy logic with analytic hierarchy process. Control. Cybern., v.35, pp.21–141.

Gupta, P. and Anbalagan, R. (1997) Landslide hazard zonation (LHZ) and mapping to assess slope stability of parts of the proposed Tehri dam reservoir, India. Quart. Jour. Engg. Geol., v.30, pp. 27-36.

Gupta, R.P. and Joshi, B.C. (1990) Landslide Hazard Zonation using the GIS Approach - A case Study from the Ramganga Catchment, Himalayas, Engg. Geol. v.28, pp.119-131.

Gupta, R.P., Saha, A.K., Arora, M.K. and Kumar, A. (1999) Landslide hazard zonation in a part of Bhagirathy Valley, Garhwal Himalayas, using integrated Remote Sensing & GIS. Jour. Him. Geol., v.20, pp.71-85.

Gupta, R.P., Kanungo, D.P., Arora, M.K. and Sarkar, S. (2008) Approaches for comparative evaluation of raster GIS-based landslide susceptibility zonation maps. Int. Jour. App. Earth. Obs. Geoinformation., v.10, pp.330-341.

Guzetti, F., Carrara, A. and Cardinali, M. and Reichenbach, P. (1999) Landslide hazard evaluation: a review of current techniques and their application in a multi-scale study, central Italy. Geomorphology, v.31, pp.181–216.

Guzzetti, F., Reichenbach, P., Cardinali, M., Galli, M. and Ardizzone, F. (2005) Probabilistic landslide hazard assessment at the basin scale. Geomorphology, v.72, pp. 272–299.

Hutchinson, J.N. (1995) Keynote paper: landslide hazard assessment. *In:* Bell (Ed.), Landslides: Balkema, Rotterdam, pp.1805–1841.

Kanungo, D. P., Arora, M. K., Sarkar, S. and Gupta, R.P. (2006) A comparative study of conventional, ANN black box, fuzzy and combined neural and fuzzy weighting procedures for landslide susceptibility Zonation in Darjeeling Himalayas. Engg. Geol., v.85, pp.347–366.

Kanungo, D. P., Arora, M. K., Sarkar, S. and Gupta, R. P. (2009) Landslide Susceptibility Zonation (LSZ) Mapping – A Review. Jour. South Asia Disaster Studies, v.2, pp.81-105.

Kanungo, D. P., Arora, M. K., Sarkar, S. and Gupta, R. P. (2009a) A Fuzzy Similarity Concept Based Rating Determination and Fuzzy Gamma Operator Based Thematic Maps Integration for Landslide Susceptibility Zonation. Georisk, v.3, pp.30-40.

Kayastha, P., Dhital, M. and De Smedt, F. (2013) Application of the analytical hierarchy process (AHP) for landslide susceptibility mapping: a case study from the Tinau watershed, west Nepal. Comput. Geosci., v.52, pp.398–408.

Kayastha, P., Dhital, M. and De Smedt, F. (2012) Landslide susceptibility mapping using the weight of evidence method in the Tinau watershed, Nepal. Nat Hazards v.63(2), pp.479–498

Kumar, R. and Anbalagan, R. (2013) Pixel based terrain analysis for Landslide Hazard Zonation, a case study of Tehri reservoir region, Uttarakhand, India, In Geos. Remote Sens. Sym. (IGARSS), IEEE, Int., pp. 2868-2871

Kundu, S., Saha , A.K., Sharma, D.C. and Pant, C.C. (2013) Remote Sensing and GIS Based Landslide Susceptibility Assessment using Binary Logistic Regression Model: A Case Study in the Ganeshganga Watershed, Himalayas. Jour. Ind. Soc. Remote Sens., v.41(3), pp.697-709

Lee, S. (2005) Application of logistic regression model and its validation for landslide susceptibility mapping using GIS and remote sensing data. Int. Jour. Remote Sens., v.26 (7), pp.1477–1491.

Lee, S. and Sambath, T. (2006) Landslide susceptibility mapping in the Damrei Romel area, Cambodia using frequency and logistic regression models. Environ. Geol., v.50, pp. 847–856.

Lee, S. and Pradhan, B. (2007) Landslide hazard mapping at Selangor, Malaysia using frequency ratio and logistic regression models. Landslides, v.4, pp.33-41.

Mathew, J., Jha, V. K. and Rawat, G. S. (2007) Weights of evidence modelling for landslide hazard zonation mapping in part of Bhagirathi valley, Uttarakhand. Curr. Sci., v.92, pp.628–638.

Mathew, J., Jha, V.K. and Rawat, G.S. (2009) Landslide susceptibility zonation mapping and its validation in part of Garhwal Lesser Himalaya, India, using Binary Logistic Regression analysis and receiver operating characteristic curve method. Landslides, v.6 pp.17-26.

Malczewski, J. (1999) GIS and multi criteria decision analysis. Wiley, New York, 408p.

Mondal, S. and Maiti, R. (2012) Landslide susceptibility analysis of Shiv-Khola watershed, Darjiling: a remote sensing & GIS based Analytical Hierarchy Process (AHP). Jour. Indian Soc. Remote Sens., v.40 (3), pp.483–496.

Nagarajan, R., Mukherjee, A., Roy, A. and Khire, M.V. (1998) Temporal remote sensing data and GIS application in landslide hazard zonation of part of Western Ghat, India. Int. Jour. Remote Sens., v.19, pp.573–585

Pachauri, A.K. and Pant, M. (1992) Landslide hazard mapping based on geological attributes. Engg. Geol., v.32, pp.81–100.

Pradhan, B. and Lee, S. (2009) Delineation of landslide hazard areas on Penang Island, Malaysia, by using frequency ratio, logistic regression, and artificial neural network models. Environ. Earth. Sci., v.60, pp.1037-1054.

Pradhan, B. and Lee, S. (2010) Delineation of landslide hazard areas using frequency ratio, logistic regression and artificial neural network model at Penang Island, Malaysia. Environ. Earth Sci., v.60, pp.1037–1054.

Pradhan, B. (2010) Remote sensing and GIS-based landslide hazard analysis and cross-validation using multivariate logistic regression model on three test areas in Malaysia. Adv. Space. Rese., v.45, pp.1244-1256.

Saaty, T.L. (1977) A scaling method for priorities in hierarchical

structures. Jour. Math. Psycho., v.15, pp.234–281.

Saaty, T.L. (1980) The analytic hierarchy process: planning, priority setting, resource allocation. McGraw-Hill International Book Company, New York.

Saha, A.K., Gupta, R.P. and Arora, M.K., (2002) GIS-based landslide hazard zonation in the Bhagirathi (Ganga) valley, Himalayas. Int. Jour. Remote Sens., v.23 (2), pp. 357–369.

Saha, A.K., Gupta, R.P., Sarkar, I., Arora, M.K. and Csaplovics, E. (2005) An approach for GIS-based statistical landslide susceptibility zonation with a case study in the Himalayas. Landslides, v.2, pp.61-69.

Sarkar, S. and Kanungo, D. P. (2004)An integrated approach for landslide susceptibility mapping using remote sensing and GIS. Photo. Engg. & Remote Sens., v.70, pp.617-625.

Sharma, S., Raghuvanshi, T. and Anbalagan,R. (1994) Plane failure analysis of rock slopes. Int. Jour. Geotec. Geol. Engg., v.13, pp.105-111.

Sharma, S., Raghuvanshi, T.K. and Anbalagan, R. (1995) Plane failure analysis of rock slopes, technical note. Geotech. Geol. Engg., v.13, pp.105–111.

Singh, T.N., Gulati, A., Dontha, L.K. and Bharadwaj V. (2008) Evaluating cut slope failure by numerical analysis—a case study. Nat Hazards, v.47, pp.263–279.

Soeters, R. and van Westen, C. (1996) Slope stability: recognition, analysis and zonation. *In:* A. Turner and R. Shuster (Eds.), Landslides: investigation and mitigation, National Academy Press, Washington, D. C., pp.129-177.

Suzen, M.L. and Doyuran, V. (2004) Data driven bivariate landslide susceptibility assessment using geographical information systems: a method and application to Asarsuyu catchment, Turkey. Engg. Geol., v.71, pp.303–321.

Valdiya, K.S. (1980) Geology of Kumaun Lesser Himalaya. Dehradun: Wadia Institute of Himalayan Geology. Interim. Report, pp. 291

van Westen, C.J., Van Asch, T.W.J. and Soeters, R. (2006) Landslide hazard and risk zonation— why is still so difûcult? Bulletin. Engg. Geol. Environ., v.65, pp.167–184.

Varnes, D.J., (1984) Landslide Hazard Zonation: A Review of Principles and Practice, Natural Hazards 3, Commission on Landslides of the IAEG, UNESCO, Paris, France, 63 p.

Watershed Management Directorate, Dehradun (2009) Report on Uttarakhand State perspective and strategic planning 2009-2027. file:///D:/For%20review/UTTARAKHAND%20SOIL.pdf

Wilson, J.P. and Gallant, J.C. (2000) Terrain Analysis: Principles and Applications," John Wiley & Sons Ltd., New York, USA, pp.1–27,

Wilson, J. (2011) Digital terrain modelling. Geomorphology, v.5, pp. 269–297.

www.digitalglobe.com/8bandchallenge - (2010)Acquisition of World view – 2 data.

Yalcin, A. (2008) GIS-based landslide susceptibility mapping using analytical hierarchy process and bivariate statistics in Ardesen (Turkey): comparisons of results and confirmations. Catena, v.72, pp.1–12.

Yesilnacar, E. and Topal, T. (2005) Landslide susceptibility mapping: a comparison of logistic regression and neural networks methods in a medium scale study, Hendek region (Turkey). Engg. Geol., v.79(3–4), pp.251–266

Zimmerman, M., Bichsel, M. and Kienholz, H. (1986) Mountain hazards mapping in the Khumbu Himal, Nepal, with prototype map, scale 1:50,000. Mountain Research and Development, v.6(1), pp.29–40.

(Received: 14 March 2014; Revised form accepted: 12 June 2014)